Cell immunolocalization of ciguatoxin-like compounds in the benthic dinoflagellate *Gambierdiscus australes* M. Chinain & M.A. Faust by confocal microscopy

Giorgio Honsell [a,*], Greta Gaiani [b], Masahiro Hirama [c], Marco Pelin [d], Aurelia Tubaro [d], Takeshi Tsumuraya [c], Mònica Campàs [b]

[a] *Department of Agrifood, Environmental and Animal Sciences - DI4A, University of Udine, via delle Scienze 91-93, Udine 33100, Italy*
[b] *Institute of Agrifood Research and Technology (IRTA), Ctra. Poble Nou km. 5.5, La Ràpita 43540, Spain*
[c] *Department of Biological Chemistry, Graduate School of Science, Osaka Metropolitan University, 1-2, Gakuen-cho, Sakai, Osaka 599-8570, Japan*
[d] *Department of Life Sciences, University of Trieste, Via E. Weiss, 2, Trieste 34128, Italy*

Keywords:
Gambierdiscus
CTX-like compounds
Immunocytochemistry
8H4 anti-CTX monoclonal antibody
Confocal microscopy

A B S T R A C T

Dinoflagellates of the genera *Gambierdiscus* and *Fukuyoa* are able to produce potent neurotoxins like ciguatoxins (CTXs), which, after biooxidation in fish, are responsible for ciguatera intoxication. An isolate of *G. australes* from the Canary Islands, that revealed the presence of CTX-like compounds by immunosensing tools, was studied by immunocytochemistry to localize intracellular CTX-like compounds, using 8H4 monoclonal antibody that specifically recognizes the right wing of CTX1B and CTX3C analogues. Confocal microscopy observations of immunostained whole cells revealed a strong positive reaction on cell surface and all along the cell outline, while no reaction was detected inside the cells, probably because the antibody was not able to pass through thecal plates. Cell sections showed a positive antibody staining not only on thecal plates, but also inside cytoplasm, with numerous small dots and larger tubule-like reticulate structures. Small fluorescent dots were detected also on the nuclear surface. These observations indicate that CTX-like compounds are present in *G. australes* cytoplasm, and then are, at least in part, released to cover the cell surface.

1. Introduction

Dinoflagellates of the genera *Gambierdiscus* and *Fukuyoa* are able to produce potent neurotoxins like ciguatoxins (CTXs), which, after biooxidation in fish, are responsible for ciguatera intoxication. *Gambierdiscus australes* was first described in the Pacific (Chinain et al., 1999; Litaker et al., 2009), and then in recent years also in other geographical areas including NE Atlantic (Fraga and Rodríguez, 2014), and the Mediterranean Sea (Tudó et al., 2020). Isolates of this species have constantly revealed CTX- and maitotoxin (MTX)-like toxicities by mouse bioassay (Chinain et al., 1999; Nishimura et al., 2013), and CTX-like activity by N2a cell-based assay (Reverté et al., 2018; Rossignoli et al., 2020). Toxin profiles obtained by LC-MS/MS are few and variable between clones, showing only in one case the presence of CTXs (Roeder et al., 2010), while in other strains CTXs were not detected, and toxins were represented by MTXs, gambierone, gambierol and gambieric acid congeners (Rhodes et al., 2014, 2017; Munday et al., 2017; Murray et al., 2019; Estevez et al., 2021).

Recently, the presence of CTX-like compounds was reported in an isolate of *G. australes* from the Canary Islands with the use of an immuno-based tool (Gaiani et al., 2020). This strategy was based on monoclonal antibodies that specifically recognize the left wing (3G8 and 10C9 antibodies) and the right wing (8H4 antibody) of CTX1B and CTX3C analogues (Tsumuraya and Hirama, 2019).

In this research the isolate of *G. australes* from the Canary Islands, that revealed the presence of CTX-like compounds by immunosensing tools, was studied by immunocytochemistry to localize intracellular CTX-like compounds by confocal microscopy.

Abbreviations: BSA, bovine serum albumin; CTX, ciguatoxin; MIP, maximum intensity z-projection; MTX, maitotoxin; PBS, phosphate buffer saline; PBT, 0.1% Triton X-100 solution in PBS; PFA, p-formaldehyde; RT, room temperature; PKS, polyketide synthase; TEM, transmission electron microscopy; WLL, white light laser; DIC, differential interference contrast; LC-MS/MS, liquid chromatography tandem mass spectrometry.

* Corresponding author.
E-mail address: giorgio.honsell@uniud.it (G. Honsell).

2. Material and methods

The study was carried out on a *G. australes* clonal culture (IRTA-SMM-16-286), isolated from the Canary Islands. Cells were grown in polystyrene flasks containing 500 mL of ES medium (Provasoli, 1968) prepared with filtered and autoclaved seawater from L'Ametlla de Mar, Spain (salinity adjusted to 36) at 24 ± 1 °C under a photon flux of 100 μmol photons m^{-2} s^{-1} with a 12:12 h light/dark regime. Cell counts were performed every 3 days until cultures reached the end of the exponential phase (200–300 cell/mL), since pellets of cultures harvested at this moment had been observed to produce CTX-like compounds (Gaiani et al., 2020).

Immunostaining was carried out on whole cells and cells sections using 8H4 anti-CTX mAb, which binds to the right wing of CTX1B, 54-deoxyCTX1B, CTX3C and 51-hydroxyCTX3C, although with different affinity constants, and lacks cross-reactivity with other related marine toxins, including brevotoxin A, brevetoxin B, okadaic acid, and MTX (Tsumuraya et al., 2006).

2.1. Whole cells protocol

Aliquots of cells were collected and pelleted at 1000 rpm for 5 min at room temperature (RT) and fixed in 4% p-formaldehyde (PFA) in phosphate buffer saline (PBS) for 30 min at RT. After 3 washes with PBS (each one of 15 min), cells were permeabilized for 30 min at 4 °C in PBT solution (0.1% Triton X-100 in PBS). Cells were then blocked for 30 min at 4 °C in a blocking solution constituted by PBT containing 1% bovine serum albumin (BSA).

Cells were then stained with 8H4 mAb, 1:500 diluted in blocking solution for 90 min at 37 °C. After 3 washes with PBT (each one of 15 min), cells were stained with secondary Alexa Fluor 488-conjugated anti-mouse IgG (Jackson ImmunoReserach; Milan, Italy), 1:500 diluted in blocking solution for 60 min at 37 °C. After 3 washes with PBT (each one of 15 min), cells were mounted on glass coverslips using ProLong™ Glass Antifade Mountant with NucBlue™ Stain for nuclei staining (Life Technologies; Milan, Italy) before confocal analysis. Alexa Fluor 488-conjugated anti-mouse IgG was used as negative control.

2.2. Cells sections protocol

Cells were fixed in 4% PFA in PBS for 30 min at RT and, after 3 washes with PBS, they were sectioned in a cryostat (5–9 μm). Then, sections were mounted on slides and immunostained following the same procedure followed for whole cells.

2.3. Confocal microscopy

Cells and sections were observed with a confocal microscope Leica TCS SP8 (Leica Microsystems GmbH, Wetzlar, Germany), using HC PL APO CS2 water immersion 40x/1.10 NA, HCX PL APO lambda blue 63x/1.40 NA and HC PL APO CS2 oil immersion 100x/1.40 NA objectives. Three laser lines were used for excitation. A diode laser at 405 nm was used for NucBlue (Hoechst 33342) excitation. Emission was detected by PMT photodetector at 411–456 nm to visualize cells nuclei. A white light laser (WLL) line at 492 nm was used for Alexa Fluor 488 conjugated IgG targeting 8H4 mAb. Emission was detected by Leica HyD hybrid photodetector at 502–543 nm with 0.3–6 ns time-gate. A WLL line at 475 nm or 580 nm was used for photosynthetic pigments excitation and emission was detected by PMT photodetector at 630–720 nm to visualize chloroplasts autofluorescence. 475 nm corresponds to the maximum absorbance region of peridinin chlorophyll *a* protein light-harvesting complex PCP (Haxo et al., 1976; Keima et al., 2000) and 580 nm corresponds to one of the absorbance maxima of chlorophylls c_1 and c_2 (Zapata et al., 2006), which characterize *Gambierdiscus* pigment composition (Durand and Berkaloff, 1985). Images reported in Figs. 3D, and 4A and 4C were acquired at 0.78 AU and 0.76 AU pinhole size, respectively, using the Leica HyVolution2 module that provides automated acquisition parameters to optimize confocal resolution (Borlinghaus and Kappel, 2016). In the case of Fig. 4A,C, images stacks were subsequently deconvolved using the integrated SVI Huygens software.

Image stacks were processed for maximum intensity z-projection (MIP) using Fiji image analysis software (Schindelin et al., 2012), and Adobe Photoshop 23.3.2 release (Adobe Inc., San Jose, California, U.S.) for illustration purposes.

3. Results

Confocal microscopy observations of *G. australes* whole cells immunostained with Alexa Fluor 488 conjugated 8H4 mAb showed a strong positive reaction on cell surface and all along the cell outline (Fig. 1A,C, D,E). Many small fluorescent dots were visible on the surface of thecal plates (Fig. 1B,C,H), matching well for position and size with thecal pores and sutures between plates, as it can be observed by differential interference contrast (DIC) images of the same cells (Fig. 1F,I). A stronger staining was observed in correspondence of the sulcus (Fig. 1A, E) and the apical pore complex (Fig. 1H). No reaction was observed inside the cell, probably because the antibody was not able to pass through thecal plates, being the Triton X-100 permeabilization approach not sufficient to allow a whole thecal permeabilization, as already reported for other dinoflagellates (Palacios and Marin, 2008). Controls, incubated with Alexa Fluor 488-conjugated secondary antibody only, were negative (Fig. 1G). The nucleus, stained by Hoechst 33342, appeared in the dorsal part of the cell. It showed a bean or elongated curved shape, and it was about 25–40 μm long and 15 μm wide. Strongly stained chromosomal structures were visible in its concave part and in some other small areas (Fig. 1A,D,G). A similar organization was observed by Cuadrado et al. (2021), who revealed by fluorescence *in situ* hybridization (FISH) that the strong staining of the concave region of *Gambierdiscus* bean-shaped nucleus corresponded to 45S rDNA clusters arranged in a large nucleolus.

Hoechst 33342 stained also a variable number (generally 15–20) of smaller highly fluorescent cytoplasmic rounded bodies with diameter between 2.5 and 7.5 μm (Fig. 1B,C). They were closer to cell surface, and on a different plane with respect to the nucleus. Analogue structures, similar in size and number, giving Feulgen and acetocarmine positive reaction, have been previously described by light microscopy, fluorescence microscopy and transmission electron microscopy (TEM) as "pseudo-nuclear vesicles" in *Gambierdiscus toxicus* (Durand and Puiseux-Dao, 1985; Durand et al., 1986).

To further investigate the presence of CTX-like compounds inside the cells, a well-established immunostaining approach on cell sections was followed. Indeed, the use of higher concentrations of Triton X-100 or an enzymatic approach to permeabilize the strong cellulosic theca (Palacios and Marin, 2008), could be applied but they could lead to strong membrane and theca structural alterations. For these reasons, these approaches were avoided. Immunostaining of cell sections showed a positive antibody staining on thecal plates, as already observed in the whole cells, and in the cytoplasm, characterized by numerous small dots and larger cytoplasmic structures (Figs. 2A–F, 3A–F and 4A–F). Small fluorescent dots were detected also on the nuclear surface (Fig. 2A,B,E). Controls, incubated with Alexa Fluor 488-conjugated secondary antibody only (Fig. 2C) or no antibody at all (Fig. 2F) were always negative. Hoechst 33342, which is a nucleic acid stain, stained not only the nucleus, but also thecal plates. Previous observations have shown that this fluorochrome is able to stain also primary plant cell walls (Hernandez and Palmer, 1988), which consist primarily of cellulose and other polysaccharides, like dinoflagellates thecal plates (Loeblich, 1970; Sekida et al., 2004). Thecal plates immunostaining evidenced a thin, almost continuous, layer on their external surface with sparse small dots and less intensely stained areas across their section (Figs. 2A,B,D,E and 3D,E). This confirmed thecal surface immunostaining observed in whole cells, suggesting a release of toxins on cell surface through thecal pores.

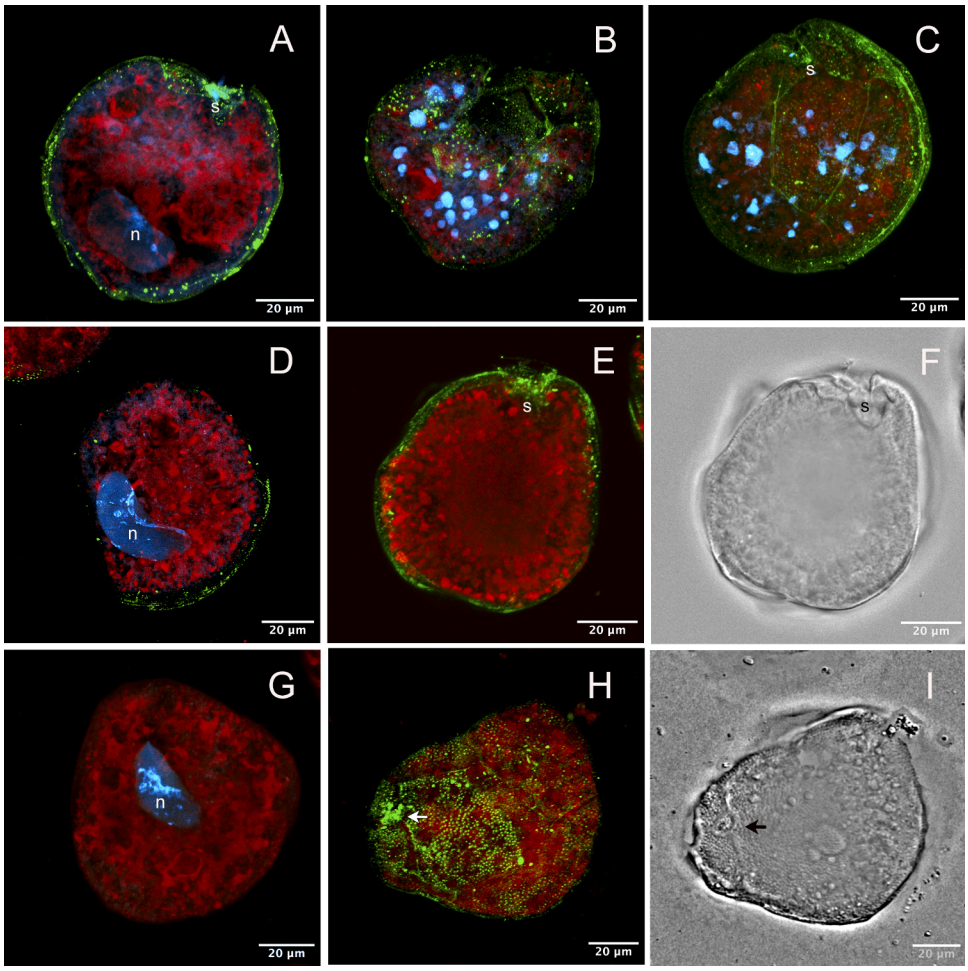

Fig. 1. *Gambierdiscus australes* (IRTA-SMM-16-286) whole cells stained with Alexa Fluor 488 coupled CTX 8H4 antibody (green fluorescence), and Hoechst 33342 (blue fluorescence) observed by confocal microscopy. Red fluorescence is given by photosynthetic pigments autofluorescence. A. Maximum intensity Z projection (MIP) of a 7 slices stack in the median part of a cell (Z thickness 4.9 µm) showing the nucleus (n) and a strong positive antibody reaction in correspondence with the girdle and the sulcus (s). B. MIP of an 11 slices stack (Z thickness 8.2 µm) of the hypothecal region of the same cell of A. Numerous Hoechst 33342 stained fluorescent bodies (pseudo-nuclear vesicles) are visible. A strong positive antibody reaction is observed with many small dots on cell surface, and in correspondence with cell margin and sutures between thecal plates. C. MIP of 20 slices (Z thickness 16.5 µm) of a cell showing pseudonuclear vesicles and positive antibody reaction at cell surface. D. MIP of 12 slices (Z thickness 4.6 µm). The nucleus (n) shows an elongated curved shape with highly fluorescent structures on its concave side. A positive antibody reaction is visible on cell margin. E. MIP of a stack of 7 slices (Z thickness 5.2 µm) showing antibody positive reaction at cell margin and at sulcus level. F. Differential interference contrast (DIC) image of the same cell showing the sulcal area where the positive antibody reaction was more intense in E. G. MIP of a stack (8 slices, Z thickness 5.9 µm) of a cell stained with Alexa Fluor 488-conjugated anti-mouse IgG and Hoechst 33342 only as negative control. No Alexa Fluor 488 staining is detectable. Only chloroplast red autofluorescence and Hoechst 33342 nuclear staining can be observed. H. MIP of a stack of 40 slices (Z thickness 22.7 µm), showing positive antibody reaction at cell surface in correspondence with thecal pores and the apical pore complex (arrow). I. DIC image of the same cell showing cell surface with thecal pores and the apical pore complex (arrow).

Numerous small fluorescent dots showing a diameter lower than 0.5 µm were observed in the cytoplasm. They were diffusely distributed, often arranged in clusters or rows, or forming a network between plastids (Fig. 2A,B,D,E). Small fluorescent dots were present also on the nuclear surface. Immunostaining also evidenced a small number (2–5 for section) of larger cytoplasmic structures with size between 6 and 8 µm (Figs. 2B, 3A–C,E,F and 4A–F). They had a globular (Fig. 4A,C) or slightly elongated (Fig. 4B) shape and appeared to be formed by short tubule-like structures arranged in a reticulate pattern. No corresponding structure was visible by light microscopy images of the same cells sections.

4. Discussion

Immunostaining of *G. australes* IRTA-SMM-16–286 clone with 8H4 anti-CTX mAb confirms the presence of CTX-like compounds in this species. Analysis of microalgal extracts of the same clone with a colorimetric immunoassay and an electrochemical immunosensor had previously indicated the presence of CTX-like compounds (Gaiani et al., 2020). CTX-like activity had been detected by N2a cell-based assay in other clones of *G. australes* from the Canary Islands and Madeira (Reverté et al., 2018; Rossignoli et al., 2020).

Previous observation on clones of this species from Pacific areas revealed both CTX- and MTX-like toxicities by mouse bioassay (Chinain et al.,1999; Nishimura et al., 2013), CTX-like activity by receptor binding assay (Chinain et al., 2010) and activity in a N2a cell-based assay, likely due to MTXs since no CTXs were detected with LC-MS/MS (Rhodes et al., 2010).

Nevertheless, LC–MS/MS analyses detected 2,3-dihydroxy P-CTX3C in an isolate from Hawaii (Roeder et al., 2010). Other isolates from the Pacific Ocean were found to produce MTX1, MTX3 and 44-methyl-gambierone and were also negative for CTXs (Rhodes et al., 2014, 2017; Munday et al., 2017; Murray et al., 2019). A *G. australes* strain from the Balearic Islands (Mediterranean Sea) showed MTX5, 44-methyl-gambierone and gambieric acids C and D, suggesting that the toxin profile of *G. australes* from the Mediterranean Sea may not be exactly the same as that observed in the same species in the Pacific Ocean (Estevez et al., 2021). Our results are a further confirmation that the analyzed strain produces compounds that have structural similarity with CTX3C and CTX1B group.

CTXs are polycyclic polyethers belonging to the family of polyketides. The polyketides biosynthetic pathway in *Gambierdiscus* and other dinoflagellates needs still to be elucidated, but recent transcriptomic and genomic studies revealed the presence of Type I modular and single domain polyketide synthases (PKSs) in *Gambierdiscus* species (Van Dolah et al., 2020). PKSs subcellular localization is still largely

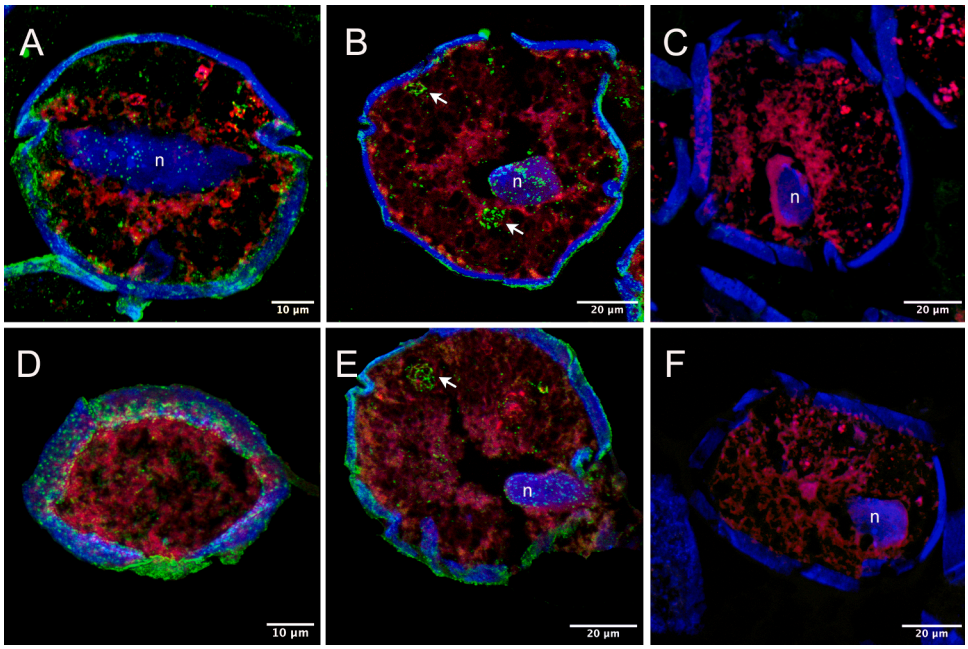

Fig. 2. *Gambierdiscus australes* (IRTA-SMM-16-286) cell sections stained with Alexa Fluor 488 coupled CTX 8H4 antibody (green fluorescence), and Hoechst 33342 (blue fluorescence) observed by confocal microscopy. Red fluorescence is given by photosynthetic pigments autofluorescence. Hoechst 33342 stains nucleus and also thecal plates. A Maximum intensity Z projection (MIP) of a stack of 23 slices (Z thickness 9.3 µm) of a longitudinal section of a cell. The nucleus is elongated and positioned in the median part of the cell. It shows a positive antibody reaction with many small dots on its surface. A positive reaction is observed also in the cytoplasm with numerous small dots arranged in clusters, and on thecal plates. B. MIP of a stack of 16 slices (Z thickness 6.3 µm) of a section of another cell showing, in addition to what observed in previous image, the immunostaining of two larger tubule-like reticulate bodies (arrows). C. MIP of a stack 18 slices (Z thickness 7.2 µm) of a cell stained with Alexa Fluor 488-conjugated anti-mouse IgG and Hoechst 33342 only as negative control. No Alexa Fluor 488 staining is detectable. D. MIP of a stack 17 slices (Z thickness 6.8 µm) of a tangential section, showing immunostaining of thecal plates with dots, probably corresponding to thecal pores, as observed in whole cells in 1B and 1H. Cytoplasmic dots appear to be arranged in clusters and rows, forming a network between plastids. E. MIP of a stack 16 slices (Z thickness 6.3 µm) of a transverse section showing the nucleus (n) and an immunostained reticulate tubule-like structure (arrow). F. MIP of 15 slices (Z thickness 5.9 µm) of a cell stained with Hoechst 33342 only as negative control.

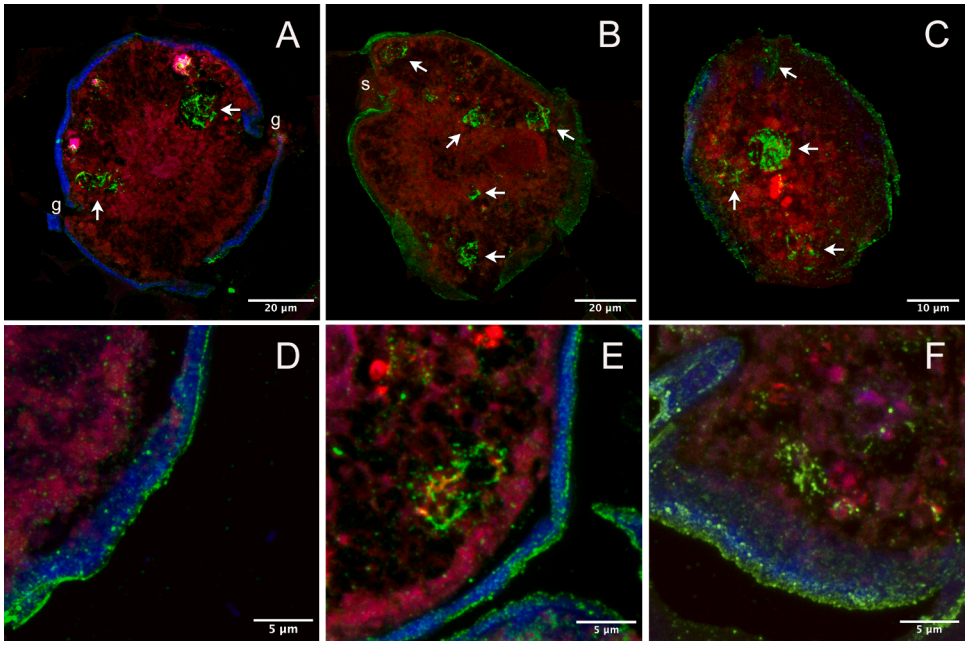

Fig. 3. *Gambierdiscus australes* (IRTA-SMM-16–286) sections immunostained with Alexa Fluor 488 coupled CTX 8H4 antibody (green fluorescence), and Hoechst 33342 (blue fluorescence) observed by confocal microscopy. Reticulate tubule-like cytoplasmic structures formed by thin filaments are visible in cell sections with a positive antibody reaction (arrows). A. Maximum intensity Z projection (MIP) of a stack of 21 slices (Z thickness 6.0 µm) of a cell longitudinal section. B MIP of a stack of 25 slices (Z thickness 8.3 µm) of a cell transverse section at sulcus (s) level. C. MIP of a stack of 26 slices (Z thickness 7.5 µm), showing a rounded reticulate structure. D. MIP of a stack of 27 slices (Z thickness 4.8 µm) in the peripheral zone of a cell showing an almost continuous immunostained layer on the outer cell surface and smaller dots on thecal plates, stained in blue by Hoechst 33342. HyVolution technique. E MIP of a stack of 29 slices (Z thickness 6.9 µm) of a section in the peripheral zone of a cell showing a large reticulate tubule-like structure and many small dots arranged in rows. F. MIP of a stack of 21 slices (Z thickness 6 µm) of a tangential section in the peripheral zone of a cell.

unknown, apart some data on *Karenia brevis, Ostreopsis* cf. *ovata* and *Coolia monotis* that indicate their localization in chloroplast and cytosol (Monroe et al., 2010; Van Dolah et al., 2013). Few data on polyether toxins localization in dinoflagellates are available: okadaic acid was found to be localized within chloroplasts of *Prorocentrum lima* and *P. maculosum* (Zhou and Fritz, 1994; Lawrence and Cembella, 1999;), and in cytoplasm (Rausch de Traubenberg et al., 1995) and cytoplasmic vacuolar structures of *P. lima* (Barbier et al., 1999), while ovatoxins showed a diffuse cytoplasmic distribution in *Ostreopsis* cf. *ovata* (Honsell et al., 2011). In *G. australes*, CTXs appear to be immunolocalized in the cytoplasm, as it occurs for ovatoxins in *O* cf. *ovata* and okadaic acid in *P. lima*, but they are found also on the external surface of thecal plates. This finding is in accordance with Campbell et al. (1987), who observed a positive anti-CTX reaction on the theca of *Gambierdiscus toxicus* cells in the gut content of herbivorous fish *Ctenochaetus strigosus*. Reticulate tubular structures evidenced in cytoplasm by immunostaining do not show any correspondence with structures observed in previous ultrastructural studies on *Gambierdiscus* (Durand and Berkaloff, 1985;

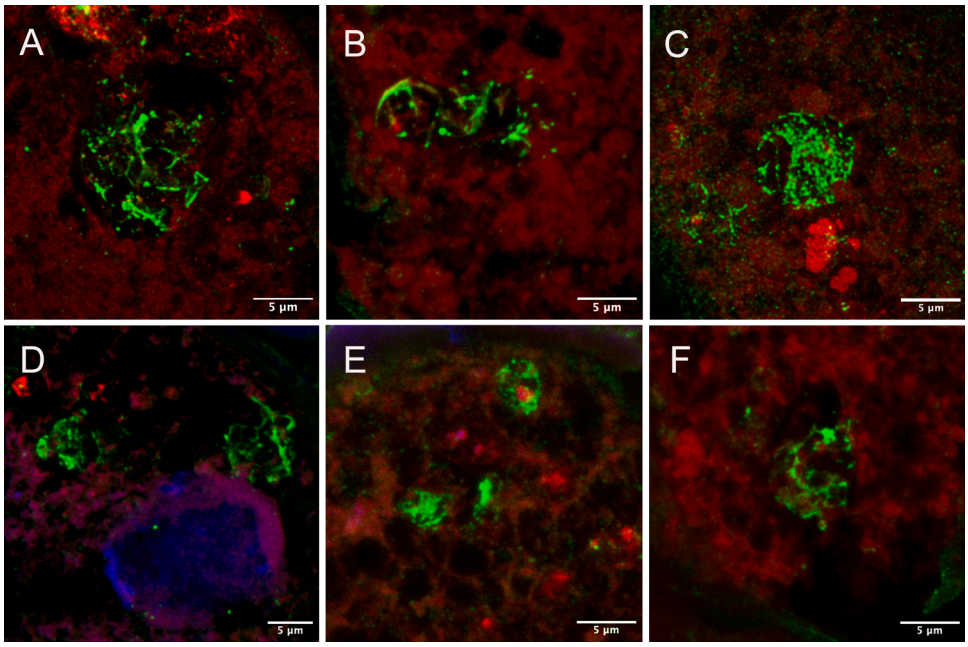

Fig. 4. Tubule-like reticulate structures in *Gambierdiscus australes* sections immunostained with Alexa Fluor 488 coupled CTX 8H4 antibody (green fluorescence) by confocal microscopy. A. Maximum intensity Z projection (MIP) of a stack of 23 slices (Z thickness 4.0 µm). HyVolution deconvolution technique. B MIP of a stack of 10 slices (Z thickness 2.7 µm) C. MIP of a stack of 16 slices (Z thickness 3.5 µm). HyVolution deconvolution technique. D. MIP of a stack of 9 slices (Z thickness 2.3 µm). E . MIP of a stack of 9 slices (Z thickness 2.3 µm). F. MIP of a stack of 7 slices (Z thickness 1.7 µm).

Durand and Berkaloff, 1985; Durand et al. 1986). The fact that these structures appear to be formed by thin tubules suggests that they could be a part of cell endomembrane system related to CTXs biosynthesis. Also scattered small dots, detected on the nuclear surface, match with a role of endomembrane system, in view of the continuity between nuclear envelope external membrane and endoplasmic reticulum. Therefore, we could hypothesize that CTXs biosynthesis takes place in the endomembrane system in cytoplasm, and then CTXs, detected as small fluorescent dots, could pass outside the cell through thecal pores, which showed a positive antibody reaction, to cover then thecal plates surface. In any case, this should be confirmed by PKSs and CTXs immunolocalization by immunoelectron microscopy. The presence of toxins on cell surface seems to be a characteristic feature of *Gambierdiscus*, not observed in other toxic benthic dinoflagellates, like *Prorocentrum* and *Ostreopsis*. This can help in understanding the role of these toxins for the ecology of *Gambierdiscus*, suggesting that their primary role could be essentially related to deter *Gambierdiscus* direct grazers or competitors by the presence of toxins on its cell surface, and their release in seawater, as detected by Solid Phase Adsorption Toxin Tracking (SPATT) technique in ciguatera areas (Roué et al., 2018, 2020). This could be an advantage for populations persisting all the year round in relatively steady conditions, as it occurs in warm seas, making ciguatera a "chronic situation" (Margalef, 1998). The following toxin accumulation and biotransformation in fish through food webs should then be considered according to the advantage given to fish by these toxic metabolites. Overall, the obtained results suggest that, to correctly identify a hotspot for ciguatera, the CTXs content should be checked in both *Gambierdiscus* cells and the marine water from which they are collected.

5. Conclusion

Immunocytochemistry allowed for the first time the intracellular localization of CTX-like compounds in a species of the genus *Gambierdiscus.* The cytoplasmic localization of CTX-like compounds suggests a role of the cell endomembrane system. Further studies directed to localize PKSs involved in CTXs biosynthesis will be necessary to better characterize toxin production in these species. The presence of CTX-like compounds on thecal surface represents a new feature, not observed before in other toxic species, and could help to understand the role of these toxins. In addition, it could allow the development of rapid and direct methods of immunodetection of toxic cells without the need of toxin extraction or cells sectioning for microscopy.

Funding

The research has received funding from the Ministerio de Ciencia e Innovación (MICIN) (Madrid, Spain), the Agencia Estatal de Investigación (AEI) (Madrid, Spain) through the CELLECTRA (PID2020-112976RB-C21) project, and European Union through the H2020 778069-EMERTOX project.

Declaration of Competing Interest

The authors declare that they have no known competing financial interests or personal relationships that could have appeared to influence the work reported in this paper.

Data availability

Data will be made available on request.

Acknowledgments

We want to thank dr. Francesca D'Este (Department of Medical Area, University of Udine, Udine, Italy) for her precious and kind assistance in confocal microscopy and prof. Stefano Pizzolitto, dr. Flavia Picco, and dr. Fabio Di Benedetto (Struttura Operativa Complessa Anatomia Patologica, Azienda Sanitaria Universitaria Friuli Centrale, Udine, Italy) for cryostat cells sectioning.

References

Barbier, M., Amzil, Z., Mondeguer, F., Bhaud, Y., Soyer-Gobillard, M.O., Lassus, P., 1999. Okadaic acid and PP2A cellular immunolocalization in *Prorocentrum lima* (Dinophyceae). Phycologia 38, 41–46.

Borlinghaus, R.T., Kappel, C., 2016. HyVolution—the smart path to confocal super-resolution. Nat. Methods 13, i–iii.

Campbell, B., Nakagawa, L., Kobayashi, M., Hokama, Y., 1987. *Gambierdiscus toxicus* in gut content of the surgeonfish *Ctenochaetus strigosus* (herbivore) and its relationship to toxicity. Toxicon 25, 1125–1127.

Chinain, M., Faust, M.A., Pauillac, S., 1999. Morphology and molecular analyses of three toxic species of *Gambierdiscus* (Dinophyceae): *G. pacificus*, sp. nov., *G. australes*, sp. nov., and *G. polynesiensis*, sp. nov. J. Phycol. 35, 1282–1296.
Chinain, M., Darius, H.T., Ung, A., Cruchet, P., Wang, Z., Ponton, D., Laurent, D., Pauillac, S., 2010. Growth and toxin production in the ciguatera-causing dinoflagellate *Gambierdiscus polynesiensis* (Dinophyceae) in culture. Toxicon 56, 739–750.
Cuadrado, A., Sixto, M., Figueroa, R.I., Bravo, I., de Bustos, A., 2021. Comparative FISH mapping of 45S and 5S rDNA in the genus *Gambierdiscus* advances understanding of the cytogenetic diversity and mitosis of dinoflagellates. Eur. J. Phycol. 57, 264–276.
Durand, M., Berkaloff, C., 1985. Pigment composition and chloroplast organization of *Gambierdiscus toxicus* Adachi and Fukuyo (Dinophyceae). Phycologia 24, 217–223.
in: Durand, M., Puiseux-Dao, S., Anderson, D., White, A., Baden, D., 1985. Physiological and ultrastructural features of the toxic dinoflagellate *Gambierdiscus toxicus* in culture. Toxic Dinoflagellates. Elsevier Science Publishing Co., Inc., pp. 61–68
Durand, M., Squiban, A., Ribier, J., Bagnis, R., Puiseux-Dao, S., 1986. Pseudonuclear vesicles in the toxic dinoflagellate *Gambierdiscus toxicus*. Biol. Cell 56, 171–180.
Estevez, P., Castro, D., Leão-Martins, J.M., Sibat, M., Tudó, A., Dickey, R., Diogene, J., Hess, P., Gago-Martinez, A., 2021. Toxicity screening of a *Gambierdiscus australes* strain from the Western Mediterranean sea and identification of a novel maitotoxin analogue. Mar. Drugs 19, 460.
Fraga, S., Rodríguez, F., 2014. Genus *Gambierdiscus* in the Canary Islands (NE Atlantic Ocean) with description of *Gambierdiscus silvae* sp. nov., a new potentially toxic epiphytic benthic dinoflagellate. Protist 165, 839–853.
Gaiani, G., Leonardo, S., Tudó, À., Toldrà, A., Rey, M., Andree, K.B., Tsumuraya, T., Hirama, M., Diogène, J., O'Sullivan, C.K., Alcaraz, C., Campàs, M., 2020. Rapid detection of ciguatoxins in *Gambierdiscus* and *Fukuyoa* with immunosensing tools. Ecotoxicol. Environ. Saf. 204, 111004.
Haxo, F., Kycia, J., Somers, G., Bennett, A., Siegelman, H., 1976. Peridinin-chlorophyll *a* proteins of the dinoflagellate *Amphidinium carterae* (Plymouth 450). Plant Physiol. 57, 297–303.
Hernández, L.F., Palmer, J.H., 1988. Fluorescent staining of primary plant cell walls using bisbenzimide (33258 Hoechst) fluorochrome. Stain Technol. 63, 190–192.
Honsell, G., De Bortoli, M., Boscolo, S., Dell'Aversano, C., Battocchi, C., Fontanive, G., Penna, A., Berti, F., Sosa, S., Yasumoto, T., Ciminiello, P., Poli, M., Tubaro, A., 2011. Harmful dinoflagellate *Ostreopsis* cf. *ovata* Fukuyo: detection of ovatoxins in field samples and cell immunolocalization using antipalytoxin antibodies. Environ. Sci. Technol. 45, 7051–7059.
Kleima, F.J., Wendling, M., Hofmann, E., Peterman, E.J.G., Van Grondelle, R., Van Amerongen, H., 2000. Peridinin chlorophyll *a* protein: relating structure and steady-state spectroscopy. Biochemistry 39, 5184–5195.
Lawrence, J.E., Cembella, A.D., 1999. An immunolabeling technique for the detection of diarrhetic shellfish toxins in individual dinoflagellate cells. Phycologia 38, 60–65.
Litaker, R.W., Vandersea, M.W., Faust, M.A., Kibler, S.R., Chinain, M., Holmes, M.J., Holland, W.C., Tester, P.A., 2009. Taxonomy of *Gambierdiscus* including four new species, *Gambierdiscus caribaeus, Gambierdiscus carolinianus, Gambierdiscus carpenteri* and *Gambierdiscus ruetzleri* (Gonyaulacales, Dinophyceae). Phycologia 48, 344–390.
Loeblich, A.R., III, 1970. The amphiesma or dinoflagellate cell covering., in: Yochelson, E.L. (Ed.), Proceedings of the North American Paleontology Convention Chicago, Illinois. Allen Press, Lawrence, Kansas., pp. 867–929.
Margalef, R., Reguera, B., Blanco, J., Fernández, M.L., Wyatt, T., 1998. Red Tides and ciguatera as successful ways in the evolution and survival of an admirable old phylum (Eds.). In: Harmful Algae, Proceedings of the of the VIII International Conference On Harmful Algae Vigo. Xunta de Galicia Intergovernmental Oceanographic Commission of Unesco, Santiago de Compostela, Spain, pp. 3–7, 25-29 June 1997.
Monroe, E.A., Johnson, J.G., Wang, Z., Pierce, R.K., Van Dolah, F.M., 2010. Characterization and expression of nuclear-encoded polyketide synthases in the brevetoxin-producing dinoflagellate *Karenia brevis*. J. Phycol. 46, 541–552.
Munday, R., Murray, S., Rhodes, L.L., Larsson, M.E., Harwood, D.T., 2017. Ciguatoxins and maitotoxins in extracts of sixteen *Gambierdiscus* isolates and one *Fukuyoa* isolate from the South Pacific and their toxicity to mice by intraperitoneal and oral administration. Mar. Drugs 15, 208.
Murray, J.S., Selwood, A.I., Harwood, D.T., van Ginkel, R., Puddick, J., Rhodes, L.L., Rise, F., Wilkins, A.L., 2019. 44-Methylgambierone, a new gambierone analogue isolated from *Gambierdiscus australes*. Tetrahedron Lett. 60, 621–625.
Nishimura, T., Sato, S., Tawong, W., Sakanari, H., Uehara, K., Shah, M.M.R., Suda, S., Yasumoto, T., Taira, Y., Yamaguchi, H., Adachi, M., 2013. Genetic diversity and distribution of the ciguatera-causing dinoflagellate *Gambierdiscus* spp. (Dinophyceae) in coastal areas of Japan. PLoS One 8, e60882.
Palacios, L., Marin, I., 2008. Enzymatic permeabilization of the thecate dinoflagellate *Alexandrium minutum* (Dinophyceae) yields detection of intracellularly associated bacteria via catalyzed reporter deposition-fluorescence *in situ* hybridization. Appl. Environ. Microbiol. 74 (7), 2244–2247.
Provasoli, L., 1968. Cultures and collection of algae. In: Proceedings of the US-Japanese Conference, Japan Society of Plant Physiology. Hakone, pp. 63–75.
Rausch de Traubenberg, C., Soyer-Gobillard, M.O., Géraud, M.L., Albert, M., 1995. The toxic dinoflagellate *Prorocentrum lima* and its associated bacteria. II. Immunolocalization of okadaic acid in axenic and non axenic cultures. Eur. J. Protistol. 31, 383–388.
Reverté, L., Toldrà, A., Andree, K.B., Fraga, S., de Falco, G., Campàs, M., Diogène, J., 2018. Assessment of cytotoxicity in ten strains of *Gambierdiscus australes* from Macaronesian Islands by neuro-2a cell-based assays. J. Appl. Phycol. 30, 2447–2461.
Rhodes, L.L., Smith, K.F., Munday, R., Selwood, A.I., McNabb, P.S., Holland, P.T., Bottein, M.Y., 2010. Toxic dinoflagellates (Dinophyceae) from Rarotonga, Cook Islands. Toxicon 56, 751–758.
Rhodes, L., Harwood, T., Smith, K., Argyle, P., Munday, R., 2014. Production of ciguatoxin and maitotoxin by strains of *Gambierdiscus australes, G. pacificus* and G. *polynesiensis* (Dinophyceae) isolated from Rarotonga, Cook Islands. Harmful Algae 39, 185–190.
Rhodes, L.L., Smith, K.F., Verma, A., Murray, S., Harwood, D.T., Trnski, T., 2017. The dinoflagellate genera *Gambierdiscus* and *Ostreopsis* from subtropical Raoul Island and North Meyer Island, Kermadec Islands. New Zeal. J. Mar. Freshw. Res. 51, 490–504.
Roeder, K., Erler, K., Kibler, S., Tester, P., Van The, H., Nguyen-Ngoc, L., Gerdts, G., Luckas, B., 2010. Characteristic profiles of Ciguatera toxins in different strains of *Gambierdiscus* spp. Toxicon 56, 731–738.
Rossignoli, A.E., Tudó, A., Bravo, I., Díaz, P.A., Diogène, J., Riobó, P., 2020. Toxicity characterisation of *Gambierdiscus* species from the Canary Islands. Toxins 12, 134 (Basel).
Roué, M., Darius, H.T., Viallon, J., Ung, A., Gatti, C., Harwood, D.T., Chinain, M., 2018. Application of solid phase adsorption toxin tracking (SPATT) devices for the field detection of *Gambierdiscus* toxins. Harmful Algae 71, 40–49.
Roué, M., Smith, K.F., Sibat, M., Viallon, J., Henry, K., Ung, A., Biessy, L., Hess, P., Darius, H.T., Chinain, M., 2020. Assessment of ciguatera and other phycotoxin-related risks in Anaho Bay (Nuku Hiva Island, French Polynesia): molecular, toxicological, and chemical analyses of passive samplers. Toxins 12, 321 (Basel).
Schindelin, J., Arganda-Carreras, I., Frise, E., Kaynig, V., Longair, M., Pietzsch, T., Preibisch, S., Rueden, C., Saalfeld, S., Schmid, B., Tinevez, J.Y., White, D.J., Hartenstein, V., Eliceiri, K., Tomancak, P., Cardona, A., 2012. Fiji: an open-source platform for biological-image analysis. Nat. Methods 9, 676–682.
Sekida, S., Horiguchi, T., Okuda, K., 2004. Development of thecal plates and pellicle in the dinoflagellate *Scrippsiella hexapraecingula* (Peridiniales, Dinophyceae) elucidated by changes in stainability of the associated membranes. Eur. J. Phycol. 39, 105–114.
Tsumuraya, T., Fujii, I., Inoue, M., Tatami, A., Miyazaki, K., Hirama, M., 2006. Production of monoclonal antibodies for sandwich immunoassay detection of ciguatoxin 51-hydroxyCTX3C. Toxicon 48, 287–294.
Tsumuraya, T., Hirama, M., 2019. Rationally designed synthetic haptens to generate anti-ciguatoxin monoclonal antibodies, and development of a practical sandwich ELISA to detect ciguatoxins. Toxins 11, 533 (Basel).
Tudó, À., Toldrà, A., Rey, M., Todolí, I., Andree, K.B., Fernández-Tejedor, M., Campàs, M., Sureda, F.X., Diogène, J., 2020. *Gambierdiscus* and *Fukuyoa* as potential indicators of ciguatera risk in the Balearic Islands. Harmful Algae 99, 101913.
Van Dolah, F.M., Zippay, M.L., Pezzolesi, L., Rein, K.S., Johnson, J.G., Morey, J.S., Wang, Z., Pistocchi, R., 2013. Subcellular localization of dinoflagellate polyketide synthases and fatty acid synthase activity. J. Phycol. 49, 1118–1127.
Van Dolah, F.M., Morey, J.S., Milne, S., Ung, A., Anderson, P.E., Chinain, M., 2020. Transcriptomic analysis of polyketide synthases in a highly ciguatoxic dinoflagellate, *Gambierdiscus polynesiensis* and low toxicity *Gambierdiscus pacificus*, from French polynesia. PLoS One 15, e0231400.
Zapata, M., Garrido, J.L., Jeffrey, S.W., Grimm, B., Porra, R.J., Rüdiger, W., Scheer, H., 2006. Chlorophyll *c* pigments: current status. Chlorophylls and Bacteriochlorophylls. Springer, Netherlands, Dordrecht, pp. 39–53.
Zhou, J., Fritz, L., 1994. Okadaic acid antibody localizes to chloroplasts in the DSP-toxin-producing dinoflagellates *Prorocentrum lima* and *Prorocentrum maculosum*. Phycologia 33, 455–461.